JOURNAL OF APPLIED POLYMER SCIENCE VOL. 12, PP. 771–788 (1968)

Prediction of Long-Term ABS Relaxation Behavior

V. E. MALPASS, *Marbon Chemical Division, Borg-Warner Corporation, Washington, West Virginia 26181*

Synopsis

The applicability of time–temperature superposition to tensile stress relaxation of ABS plastics has been verified at strains from 0.5 to 5% for temperatures in the range of 10–50°C. Master curves have been compiled to predict the long-term stress relaxation at 23°C. and a stress–strain–reduced time surface has been constructed. A comparison of relaxation times and activation energies has confirmed that a strain increase facilitates stress relaxation up to yield. The decay of relaxation modulus at linear viscoelastic strains was shown to be equivalent to that of tensile creep modulus. By normalizing the master curves to originate at yield stress and then converting them into multiaxial form the strain which gives the best data fit with long-term hydrostatic pipe-burst strength was shown to be at yield or beyond. The ABS yield-strain master curves at 23°C. were shown to match satisfactorily the long-term pipe-rupture data. Activation energies for ABS relaxation have been compared below and above the rigid-matrix T_g, to assess the degree of stiffening of the polymer in the solid state.

INTRODUCTION

ABS plastics are used in a variety of engineering applications, where long-term mechanical performance is a prime factor which requires supporting laboratory characterization. Many established procedures for measuring the long-term mechanical performance of plastics are time-consuming and involve relatively large quantities of material. The time requirements for evaluating long-term relaxation characteristics are substantially reduced if the technique of time–temperature superposition can be used for constructing a relaxation master curve at the reference temperature.[1,2] The time–temperature superposition principle is applicable if there is a constant distribution of relaxation mechanisms over the temperature range of the measurements. The stress relaxation of ABS plastics would be expected to depend in some degree on the elastomeric content, the molecular structure, and the interface association of the copolymer matrix and elastomeric phase. Long-term stress relaxation at room temperature is governed by the slower molecular relaxations of the rigid copolymer. Above the glass-transition temperature T_g of the copolymer all relaxation mechanisms are of a rubbery type, and the polymer interactions will have changed. Consequently, time–temperature superposition involving these higher temperatures would not be expected to give a correct prediction of room-temperature behavior. A temperature limit

has to be imposed to prevent incorrect predictions of room-temperature properties.

Ferry[3] has refined the earlier empirical superposition methods of Leaderman and Tobolsky into the method of reduced variables, which requires that the stress during stress relaxation be reduced to the form $S(t)\rho_0 T_0/\rho T$ to account for a small vertical shift due to a temperature and density change from T_0 and ρ_0 to T and ρ, respectively. This correction recognizes the entropy-spring nature of the stored elastic energy. The superposed master curve at the reference temperature T_0 is constructed by shifting the curves of reduced stress at higher temperatures horizontally to the right by $\log a_T$, where a_T is the superposition shift factor. Stress relaxation is then in terms of the logarithm of reduced time, $\log a_T t$. The Rouse flexible-chain theory[4] applied to an undiluted polymer supports the reduced variable approach by showing the significance of the shift factor a_T in terms of polymer viscosity. The ratio of any relaxation time $\tau(T)$ at temperature T to the corresponding relaxation time $\tau(T_0)$ at some reference temperature T_0 is

$$\tau(T)/\tau(T_0) = \eta\rho_0 T_0/\eta_0 \rho T = a_T \tag{1}$$

where η and η_0 are the polymer viscosities at temperatures T and T_0, respectively.

The validity of applying time–temperature superposition to ABS systems has been evaluated at different strains to beyond yield, and the 23°C. long-term stress relaxation has been characterized in terms of a stress-strain–reduced time surface. The significance of stress relaxation at yield strain in relation to multiaxial-failure analysis has been described previously for metals[5] and polymers.[6] Measurements of the circumferential strain during short-term pipe bursting have been made to confirm that ABS pipe will rupture near yield strain. The 23°C. long term pipe rupture stress has therefore been evaluated by converting the yield stress master curve into multiaxial form, which has then been compared with experimental long-term data.

An estimate of the difference in polymer segmental mobility at room temperature and in the polymer melt has been derived by comparing the apparent activation energy for stress relaxation at strains greater than yield with the corresponding apparent activation energy for melt flow at very low shear rate.

EXPERIMENTAL

Materials

Two ABS graft copolymers based on the same diene were analyzed for relaxation characteristics. ABS I is representative of the high diene extrusion grades and contains more diene than ABS II by a factor of 2.3. Each ABS plastic contains a combination of colorants, antioxidants, and processing aids equivalent to those in the corresponding pipe products.

The plastics were compounded by melt-mixing in a Banbury mixer followed by milling on a two-roll rubber mill.

Specimens

ABS I tensile specimens were injection-molded at 280°C. and 1300 psi from pellets dried at 90°C., and ABS II tensile specimens were prepared by both injection-molding at 255°C. and 1300 psi and machining from a slab compression-molded at 170°C. with no dwell time. All specimens were prepared in accordance with ASTM D638-64T specifications and conditioned according to ASTM D618-61 Procedure A.

Stress Relaxation

The decay of nominal tensile stress was recorded as pounds per square inch over a 100 min. period at different temperatures and 50% relative humidity on a Model TT Instron testing machine. The Instron was calibrated for use with a strain-gage extensometer at each temperature. The temperature variation throughout the measuring period was controlled to better than ±0.5°C. by means of an Instron environmental test chamber.

The required strain in the calibrated central 2 in. region of the tensile bar was obtained by applying the necessary stress, which was first calculated from the appropriate mean stress–strain curve. Each tensile bar was allowed 15 min. at the test temperature to attain thermal equilibrium. At least two tensile bars were strained to break at each test temperature at a constant strain rate of 5%/min. (0.2 in. crosshead travel per 4 in. jaw separation per minute).

The stress relaxation of annealed ABS I tensile bars was measured at temperatures (°C.) of 10, 23, 30, 38, 43, and 49 at strains (%) of 0.5, 0.75, 1.0, 1.5, 2.0, 2.5, 3.0, 4.0, and 5.0. Zero time was measured as the instant the crosshead was stopped at the applied strain. For ABS II the stress relaxation was measured at temperatures in the range 23–82°C. at yield strain only.

Short-Term Pipe-Rupture Test

The ASTM D1599-62T test method was used for measuring ABS extruded pipe-burst strength at short times, of the order of 1–2 min. By varying the rate of pressure increase pipe-burst times corresponding to the tensile yield times were obtained. The pipe-test specimens were 18 in. in length, cut from 1 in., schedule 40, extruded pipe. All pipe specimens were conditioned at 23°C. for a minimum of 1 hr. prior to testing and were tested for pressure leaks. The pressurized pipe was clamped in a horizontal position in a constant-temperature water tank. The circumferential strain was measured up to rupture by means of a mirror and cathetometer focused on the pipe at the most likely burst point.

Long-Term Hydrostatic Pipe-Burst Test

The ASTM D1598-63T procedure was used for evaluating the time to failure under continuous hydrostatic pressure of 18 in. lengths of 1 in. schedule-40 extruded pipe. All specimens were immersed in a circulating water tank controlled at 23 ± 1°C. Each specimen was allowed a minimum of 24 hr. at 23°C. before being pressurized.

Melt Extrusion

A Merz-Colwell type of rheometer was used in conjunction with the Instron Tensile Tester to give polymer melt-flow data in the 200–300°C. range. A proportioning rate and reset control system maintained the temperature to within ±0.5°C. The ABS was predried at 88°C. for 4 hr. in a circulating air oven prior to extrusion through a 2-in. tungsten carbide capillary with a diameter of 0.060 in. and a 90° entrance angle. Extrusion rates were varied to give apparent shear rates of 1.7–1740 sec.$^{-1}$.

ANNEALING OF ABS RESINS

A major factor governing stress relaxation is the residual stress in the test specimen, which varies according to the method of preparation.[7] The annealing conditions for injection-molded tensile bars were determined by measuring dimensional stability, density, weight loss, stress–strain dependence at 23°C., and stress relaxation at 23°C. and 1% strain as a function of annealing under nitrogen. The specimens were supported between glass plates during annealing so as to minimize warping. Annealing temperatures in the range 70–115°C. were evaluated by using a 12 hr. annealing time. This period was found to produce a maximum increase in heat-distortion temperature. The results showed that temperatures within ±10°C. of the 264 psi ASTM heat-distortion temperature gave the greatest reduction in the residual stress while not causing any measurable degradation or warping. ABS I and II tensile specimens were therefore annealed at the heat-distortion temperature of 93°C. for 12 hr.

STRESS RELAXATION OF ABS I

The stress relaxation data for annealed ABS I have been satisfactorily superposed to give a 23°C. master curve for each strain of temperature-reduced stress $S(t)T_0/T$ versus logarithm of reduced time, log $a_T t$, from 10^{-2} min. to beyond 10^6 min. The vertical shift factor has been simplified to T/T_0, because the density change is insignificant in ABS polymers over the narrow experimental temperature range. The 100 min. reduced stress relaxation curves are nearly linear after the initial 3 min. The long-term relaxation behavior is based on the superposition of the portion of the relaxation curves from 3 to 100 min. The set of semilogarithmic master curves obtained in this way for annealed ABS I is represented in Figure 1, which shows the three-dimensional relationship between temperature-

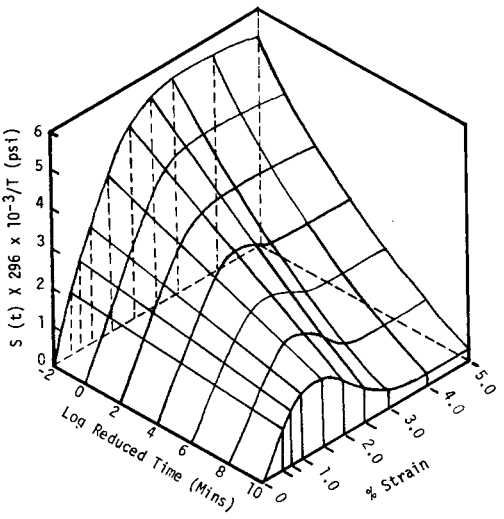

Fig. 1. Stress–strain–reduced-time surface of annealed ABS I at 23°C.

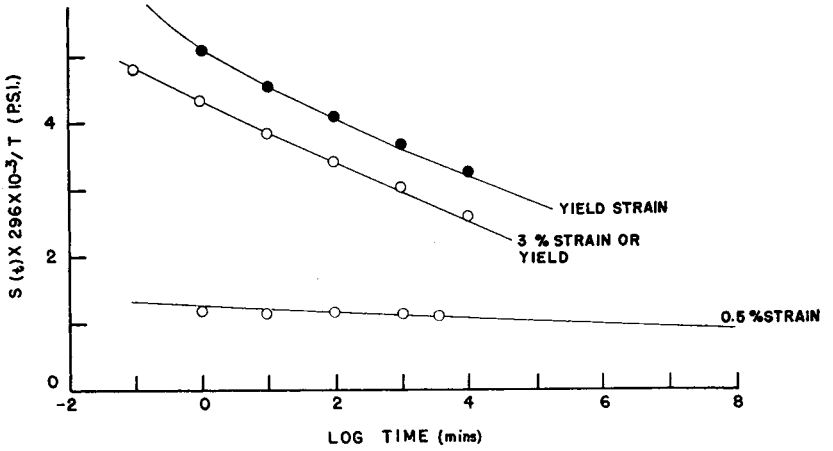

Fig. 2. Comparison of (——) stress-relaxation master curves reduced to 23°C. and experimental long-term stress relaxation at 23°C.: (○) experimental annealed ABS I stress values; (●) experimental annealed ABS II stress values.

reduced stress, per cent strain, and reduced time at 23°C. The isochronal stress–strain curve exhibits a maximum, which at 0.1 min. is indefinable at 3% strain but becomes more accentuated with time, so that at 10^6 min. it is well defined at 1.9%. These maxima appear as a ridge on the stress–strain–time surface. At strains beyond this ridge the surface flattens out owing to the similarity of the relatively rapid stress decay beyond 3% strain. This flat portion has been found to be suitable for predicting long-term pipe rupture. The surface is a mechanical fingerprint establishing the linear viscoelastic region and also describing the long-term stress relaxation

at higher strains and temperatures from 10 to 50°C. A linear viscoelastic response is obtained at strains of less than 1% to times beyond 10^6 min.

The master curves must match the actual 23°C. stress relaxation over the same time scale, if time–temperature superpositioning is valid. To evaluate the equivalence of superposed and long-term stress relaxation, the 23°C. stress relaxation of annealed ABS I was measured over five decades of time at 0.5 and 3.3% strains. Figure 2 shows that master curves compiled by time–temperature superpositioning satisfactorily predict long-term relaxation at each strain level. The 23°C. master curve compiled from constant 3% strain data is indistinguishable from the yield-strain

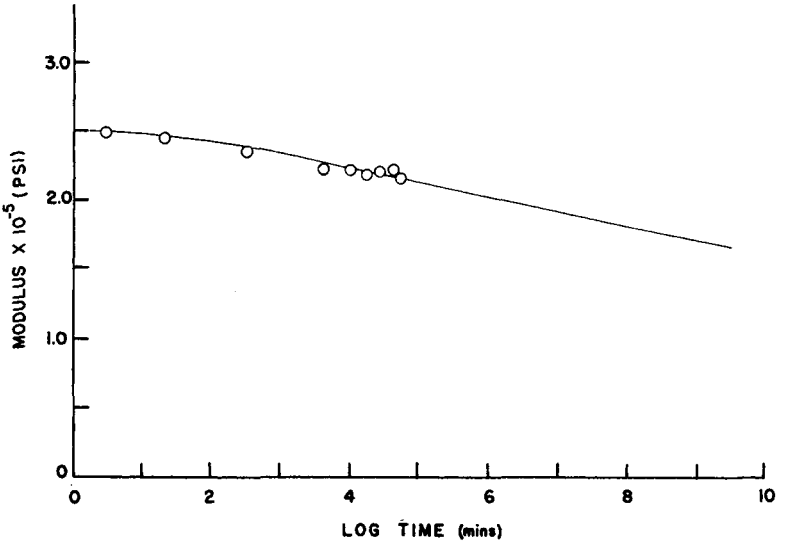

Fig. 3. Equivalence of ABS I apparent tensile creep modulus and superimposed apparent stress-relaxation modulus decay at 23 C.: (O) experimental creep modulus data at approximately 0.5% strain; (——) superposed tensile relaxation modulus curve at 0.5% strain.

master curve (3.3% at 23°C., dropping to 2.9% at 49°C.). The accuracy of predicting annealed ABS II stress relaxation at yield strain is also shown in Figure 2.

McLeod[8] has demonstrated the equivalence of stress relaxation and tensile creep at linear strains for a number of amorphous and semicrystalline polymers. To evaluate this equivalence for ABS polymers, the curve of superposed apparent stress relaxation modulus calculated for ABS I at 0.5% strain has been compared with experimental apparent creep modulus values at 1000 psi (approximately 0.5% strain). Figure 3 shows that the creep data are satisfactorily described by the stress-relaxation curve over five decades of time. Consequently, long-term ABS tensile creep can be calculated directly from short-term superposed stress relaxation over this time scale, if the linear viscoelastic limit is not exceeded.

ABS STRESS-RELAXATION MECHANISM

Because the relaxation measurements were made below the styrene–acrylonitrile copolymer T_g, the free-volume treatment and the Williams-Landel-Ferry equation[9] would not be expected to apply. The presence of an elastomeric graft phase will moderate the relaxation of the rigid copolymer molecules.

ABS stress relaxation can be compared with that of poly(methyl methacrylate), PMMA, below its α transition temperature when the β mechanism is operating. The α process is due to segmental motion of the polymer backbone chain, which should be similar to the corresponding processes in the styrene–acrylonitrile copolymer component of an ABS resin. The β mechanism is attributed mainly to rotation of the whole PMMA side group about the C—C bond as axis. A qualitative comparison may be made between the β mechanism and the mobile diene relaxation mechanism in ABS. The molecular motion responsible for the α process has an apparent activation energy, ΔH_a of 30–300 kcal./mole,[10] as compared

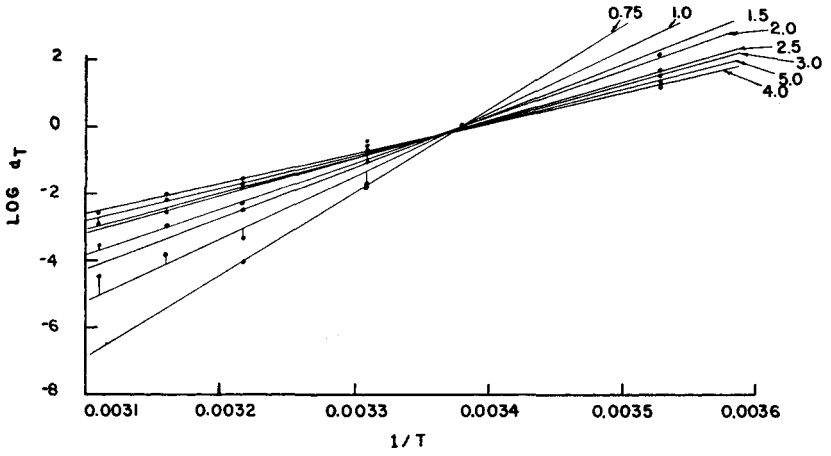

Fig. 4. Arrhenius plots for annealed ABS I at strains up to and beyond yield.

with 20 kcal./mole for the β process,[11] at temperatures not much lower than T_g. In this temperature region the α response controls the long-term relaxation, and the superposition procedure is still valid. The shorter time response will be governed by the rapid β process and will not superpose, but this limitation does not prevent superposition of the long-term relaxation data. The α process follows an Arrhenius dependence of a_T on temperature below T_g, so that

$$(d \ln a_T)/d(1/T) = \Delta H_a/R \quad (2)$$

The β process in PMMA will conform to the WLF equation. However, in the ABS system it is not side groups which are mobile, but a second backbone chain. The T_g of the diene phase is of the order of $-90°$C.,

which means that the stress relaxation measurements are made above the $(T_g + 100)$ range of the rubber. Consequently, an Arrhenius equation should also apply to the rubber relaxation. Below the α transition temperature of 105°C. PMMA does conform to an Arrhenius equation.[12] By straining to yield, an acceleration of the α process has been observed for poly(ethyl methacrylate),[13] which is comparable to that caused by heating to T_g and should apply to ABS. It has also been established that a simple Arrhenius relationship is applicable to superposition of semicrystalline polymers well below their melting point: ΔH_a values of 30, 125, and 88 kcal./mole have been measured for polyethylene,[14] polychlorotrifluoroethylene,[15] and nylon,[16] respectively.

Figure 4 shows that an Arrhenius a_T dependence on temperature applies to the ABS system at strains from within the linear limit to beyond yield. The ΔH_a values for ABS fall within the range reported for rigid or semicrystalline polymers. A decrease in ΔH_a as strain increases is consistent with strain expanding the polymer matrix. The expansion would be expected to occur mainly in the rigid copolymer under the influence of a triaxial stress field, which is a direct consequence of the difference in Poisson's ratio of the copolymer matrix and elastomeric phase.[17] Table I contains the a_T and ΔH_a data calculated for ABS I at each strain.

TABLE I
Dependence of Log a_T on Temperature
as a Function of Strain for Annealed ABS I

Strain, %	Temperature, °K.						ΔH_a, kcal./mole
	283	296	303	311	316	322	
0.75		0	−1.64	−4.07			117
1.0		0	−1.69	−3.34	−3.71	−4.46	81
1.5		0	−1.04	−2.43			69
2.0	2.17	0	−0.68	−2.30	−3.00	−3.55	62
2.5	1.64	0	−0.43	−1.76			48
3.0	1.47	0	−0.43	−1.89	−2.58		44
4.0	1.20	0	−0.57	−1.66	−2.07	−2.65	43
5.0	1.27	0	−0.65	−1.62	−2.24	−2.93	44

A simplified approach to calculating and comparing the relaxation times of ABS plastic at different strains is to assume that the Maxwell-Wiechert model predicts the relation of relaxation modulus $E_r(t)$ versus time t at constant strains within the linear limit of viscoelasticity.

If a discrete set of relaxation times $\tau_1, \tau_2, \tau_3, \ldots \tau_n$ describes the stress relaxation process, then

$$E_r(t) = E_\infty + \sum_{i=1}^{n} E_i \exp \{-t/\tau_i\} \tag{3}$$

were τ_i is the relaxation time for modulus increment E_i and E_∞ is the ultimate rubbery modulus.

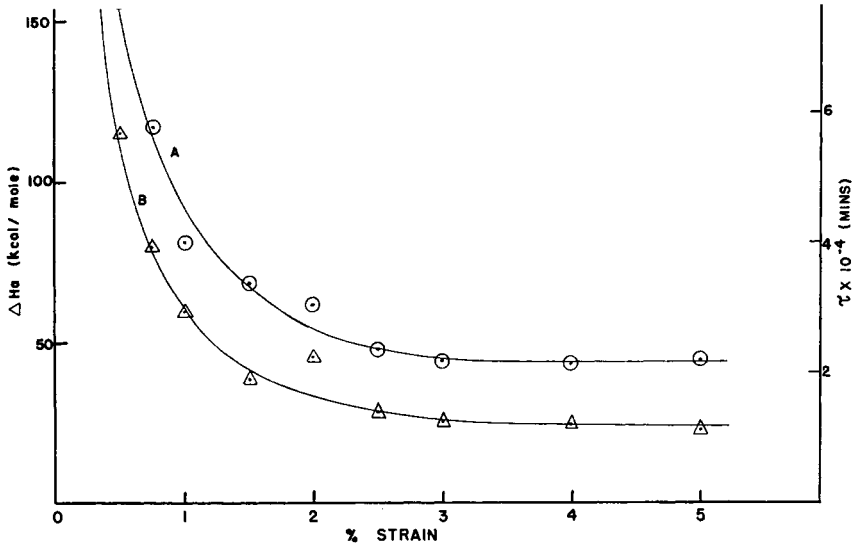

Fig. 5. Relaxation parameters of annealed ABS I as a function of per cent strain: (*A*) variation of ΔH_a; (*B*) variation of τ.

The condition of discrete or single relaxation times applies if log $E_r(t)$ is in part, a linear function of t. Landel and Stedny[18] have shown that, time–temperature superposition may be extended to stress relaxation in pure SBR rubbers at large deformations by defining a strain-reduced modulus $E_r^*(t) = E_r(t)f(\alpha)$, where $f(\alpha)$ is a function of extension ratio α as obtained from the Martin-Roth-Stiehler equation.[19] It has been assumed in the present investigation involving strains up to only 5% that $f(\alpha)$ is independent of time and temperature over the 100 min. period and 39°C. temperature range. Linear plots of log $E_r(t)$ versus time have been obtained for ABS I at all strains up to and beyond yield for the relatively short period from 400 to greater than 1000 min. The relaxation time corresponding to this restricted linear portion of each plot of log $E_r(t)$ versus time has been calculated for each strain, assuming a constant $f(\alpha)$ at the small strains involved. The values of the calculated modulus at the higher strains may be in error, but the relaxation times will be correct if the assumptions concerning $f(\alpha)$ are valid.

Both curves A and B in Figure 5 indicate that the relaxation process becomes progressively easier and faster as strain is increased. This effect of strain in reducing the viscoelastic relaxation times and causing a lowering of glass temperature has been previously well established.[13,20] Beyond 3% strain (yield) there is almost no change in the relaxation parameters, which proves that relaxation of stress attains a maximum rate which is maintained beyond yield up to rupture. It is likely that the rigid-copolymer free volume reaches a maximum at yield strain and thereafter remains unchanged up to fracture.

CONVERSION OF SUPERPOSED TENSILE STRESS INTO MULTIAXIAL PIPE-BURST STRESS

The yield characteristics of many metals and plastics under combined stress situations have been satisfactorily described by the von Mises[5,6] failure condition:

$$(S_1 - S_2)^2 + (S_2 - S_3)^2 + (S_3 - S_1)^2 = 2S_T^2 \quad (4)$$

where S_1, S_2, and S_3 are the three principal stresses in the system, and S_T is the yield stress in tension. This relationship predicts that the Barlow hoop stress in a thin-wall closed-end pipe at the time of failure is 16% greater than the tensile yield stress. The von Mises proportionality constant approaches unity if the pipe specimen is under any additional longitudinal stress. The Tresca failure condition[5,6] also predicts an equality between hoop stress and tensile yield stress.

The hoop stress in a pipe is a function of internal pressure P_i, external diameter D, and wall thickness t. Barlow hoop stress is calculated from the simple relationship

$$S_{\text{hoop}} = P_i D/2t \quad (5)$$

where $D/t > 10:1$ for thin-wall pipe.

The International Standards Organization (ISO) hoop stress is calculated from the more expanded equation[21]

$$S_{\text{hoop}} = P_i(D - t)/2t \quad (6)$$

The ISO hoop stress is approximately 10% lower than the Barlow hoop stress for thin-wall pipe and should be 4% greater than tensile yield stress, according to the von Mises yield condition.

Baer et al.[22] used the von Mises criterion to convert satisfactorily the room-temperature long-term stress relaxation at yield strain of a low-density polyethylene into long-term Barlow pipe-rupture stress. Faupel[23] also has accurately calculated both short- and long-term rupture stress of rigid poly(vinyl chloride) pipe by applying the von Mises failure concept. The 23°C. stress-relaxation master curves obtained for ABS I at strains from 0.5% to beyond yield have therefore been used as the basis for predicting long-term pipe rupture first by normalizing to commence at yield stress and then by converting into hoop stress. The requirement that short-term pipe rupture of ABS I occurs at yield strain has been confirmed by measuring the circumferential pipe strain at the same rate as that used for imposing yield strain in the stress-relaxation measurements. Each master curve is normalized by multiplying the data points by a constant factor (NF), which is the ratio of the 23°C. stress at yield strain at zero relaxation time to the corresponding stress at the applied strain, both strains being applied at the same rate. The conversion of the normalized master curves at yield strain into multiaxial form is achieved by multiplying the normalized data points by a constant multiaxial conversion factor (MCF). This

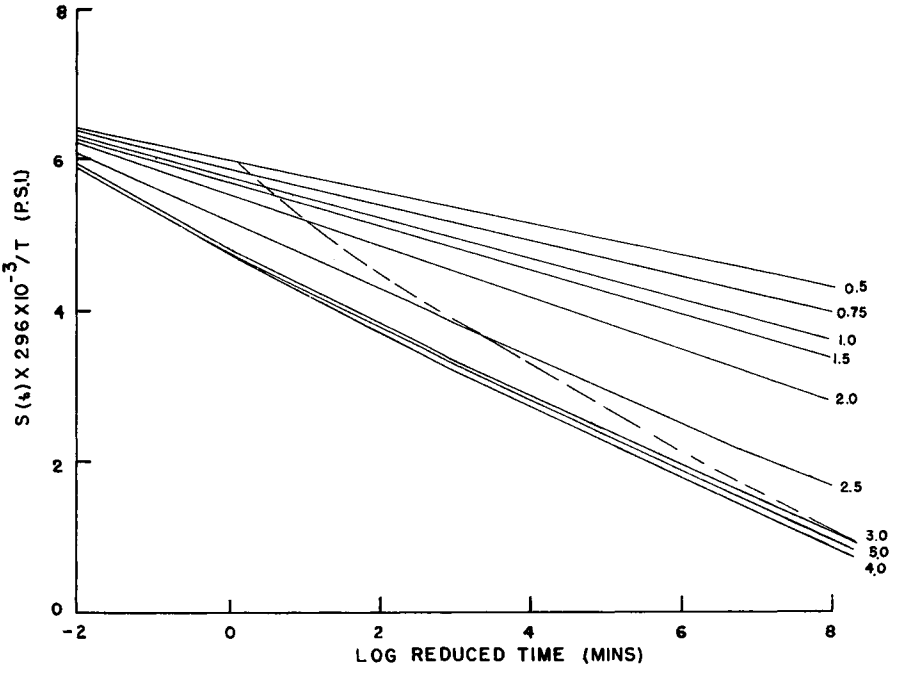

Fig. 6. Comparison of (——) multiaxially converted, normalized ABS I master curves and (– – –) long-term pipe-rupture stress at 23°C. Each master curve is identified by per cent strain.

factor is determined experimentally by dividing the appropriate short-term hoop stress by the tensile yield stress, both stresses being measured at a strain rate of approximately 5%/min. Table II contains the normalizing and multiaxial conversion factors used for converting the ABS I master curves into Barlow pipe-burst form. The MCF was 1.07, which is intermediate between the factors predicted by the von Mises and Tresca failure criteria, when no additional longitudinal stress is present.

TABLE II
ABS I Normalization and Multiaxial Conversion Factors[a]

Strain, %	Initial applied stress, psi	NF	NF × MCF
0.5	1,282	4.37	4.68
0.75	1,964	2.68	3.06
1.0	2,572	2.18	2.34
1.5	3,650	1.54	1.65
2.0	4,594	1.22	1.31
2.5	5,230	1.07	1.15
3.0	5,594	1.00	1.07
4.0	5,466	1.03	1.10
5.0	5,215	1.08	1.15

[a] MCF = 1.07

Figure 6 shows the set of converted master curves obtained for annealed ABS I from 10^{-1} min. up to 10^{8} min., together with the appropriate statistical pipe-burst stress-decay curve. The best fit with the pipe-burst curve at times greater than 1000 hr. is given by the converted 3% relaxation plot. There is, however, very little difference between the 3, 4, and 5% converted stress-relaxation curves. The portion of the stress–strain–time surface which best defines pipe-burst behavior is therefore at yield strain and up to strains near break. The molecular structure of the ABS resin in the annealed tensile specimens at yield strain or beyond must therefore be very similar to the molecular structure existing in the pipe at the point of rupture.

A true yield-strain master curve was constructed as a check on the significance of a variable strain (2.9–3.3%) with respect to predicting long-term hydrostatic pipe rupture. Figure 2 shows that the master curve was indistinguishable from the constant 3% strain master curve: ΔH_a for relaxation at yield strain is 43 kcal./mole, compared with 44 kcal./mole at constant 3% strain.

EFFECT OF ANNEALING ON PIPE-BURST PREDICTION OF ABS II

The effect on stress relaxation of annealing differently prepared tensile specimens is shown in Figure 7. The 23°C. master curves at yield strain of the unannealed specimens decay more rapidly than the corresponding 93°C. annealed bars. The prediction of long-term pipe-burst stress from

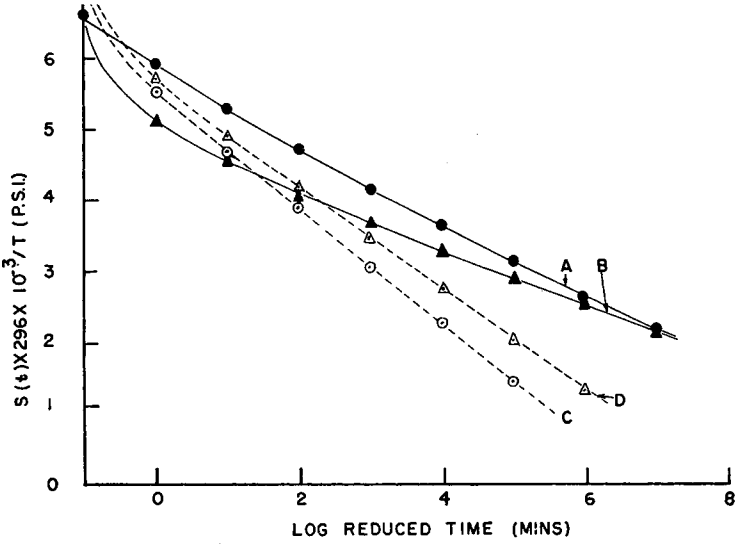

Fig. 7. Comparison of long-term stress relaxation of 23°C. of unannealed and annealed ABS II: (*A*) annealed, injection-molded; (*B*) annealed, compression-molded; (*C*) unannealed, injection-molded; (*D*) unannealed, compression-molded.

stress-relaxation data on unannealed specimens would be considerably lower than the measured pipe-burst data. These observations are consistent with the curves of stress versus strain when a faster decay of stress with applied strain is demonstrated with unannealed ABS. The stress–strain and stress-relaxation data indicate that the use of unannealed tensile specimens in predicting pipe-burst stress is not feasible, irrespective of the method of preparation. This observation is not unexpected, because the pipe extrusion technique combined with the strain and length of time involved in pipe-burst testing are all conducive to pipe-annealing. In terms of polymer structure, a state of maximum entropy or minimum orientation must exist during the tensile test at yield strain to reproduce the relaxation mechanism operating during pipe yielding.

The relaxation procedure describes the basic molecular structure but does not account for anisotropy produced in the pipe by processing conditions. The fact that the stress-relaxation specimens have to be annealed implies that a relatively unstrained state exists in the extruded pipe. Any external influences, such as chemical attack or degradation, are not predicted by the conventional relaxation experiment, unless suitable environmental conditions are used.

APPARENT ACTIVATION ENERGY ΔH_a FOR ABS II STRESS RELAXATION

Figure 8 shows the Arrhenius dependence of log a_T on the reciprocal of temperature for both unannealed and annealed ABS II prepared by injection-molding and machining compression-molded sheet. Table III contains the shift factor and apparent activation energy data at yield strain for the different specimens.

Linearity is satisfactorily defined for each type of specimen up to 50°C. The shift factors calculated for the annealed injection-molded ABS at 71 and 82°C. fell below the extrapolated Arrhenius line. If the stress-relaxation data at these higher temperatures are included in the master

TABLE III
Dependence of a_T and ΔH_a on Specimen Preparation for ABS II

Temp. T, °K.	$1/T$	Unannealed, log a_T		Annealed, log a_T	
		Inj. mold	Comp. mold	Inj. mold	Comp. mold
296	0.00338	0	0	0	0
303	0.00331	−0.22	−0.86	−0.75	−1.03
311	0.00322	−1.05	−1.56	−1.52	−2.07
316	0.00316	−1.81	−2.48	−2.43	−3.10
322	0.00311	−2.33	−3.02	−3.27	−3.85
333	0.00300			−4.75	
344	0.00291			−6.10	
355	0.00282			−7.12	
ΔH_a, kcal./mole:		40	50	57	66

curve, a low pipe-burst prediction is obtained. The activation energy is lower for the injection-molded specimens: annealing has increased ΔH_a by 17 kcal./mole for the injection-molded specimens and by 16 kcal./mole for the compression-molded specimens.

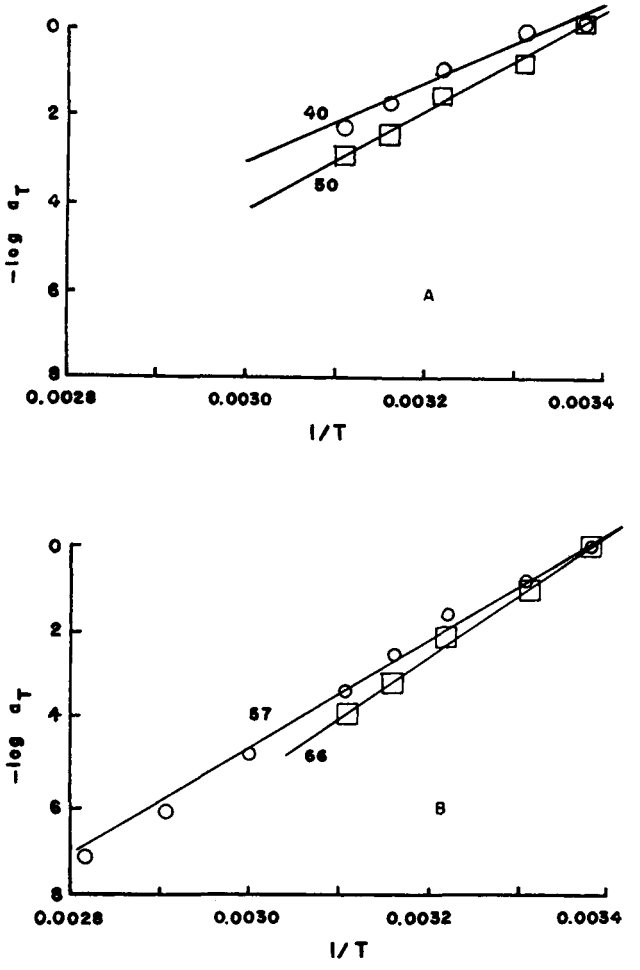

Fig. 8. Arrhenius plots of ABS II resin, (*A*) unannealed and (*B*) annealed, at yield strain: (O) injection-molded; (□) compression-molded. The apparent activation energy ΔH_a (kcal./mole) is shown for each plot.

The ΔH_a at yield strain for annealed injection-molded ABS II is approximately 13 kcal./mole greater than the corresponding value for annealed ABS I shown in Table I. This means that ABS II has a structure which is more resistant to cold flow below the T_g of the non-elastomeric copolymer matrix.

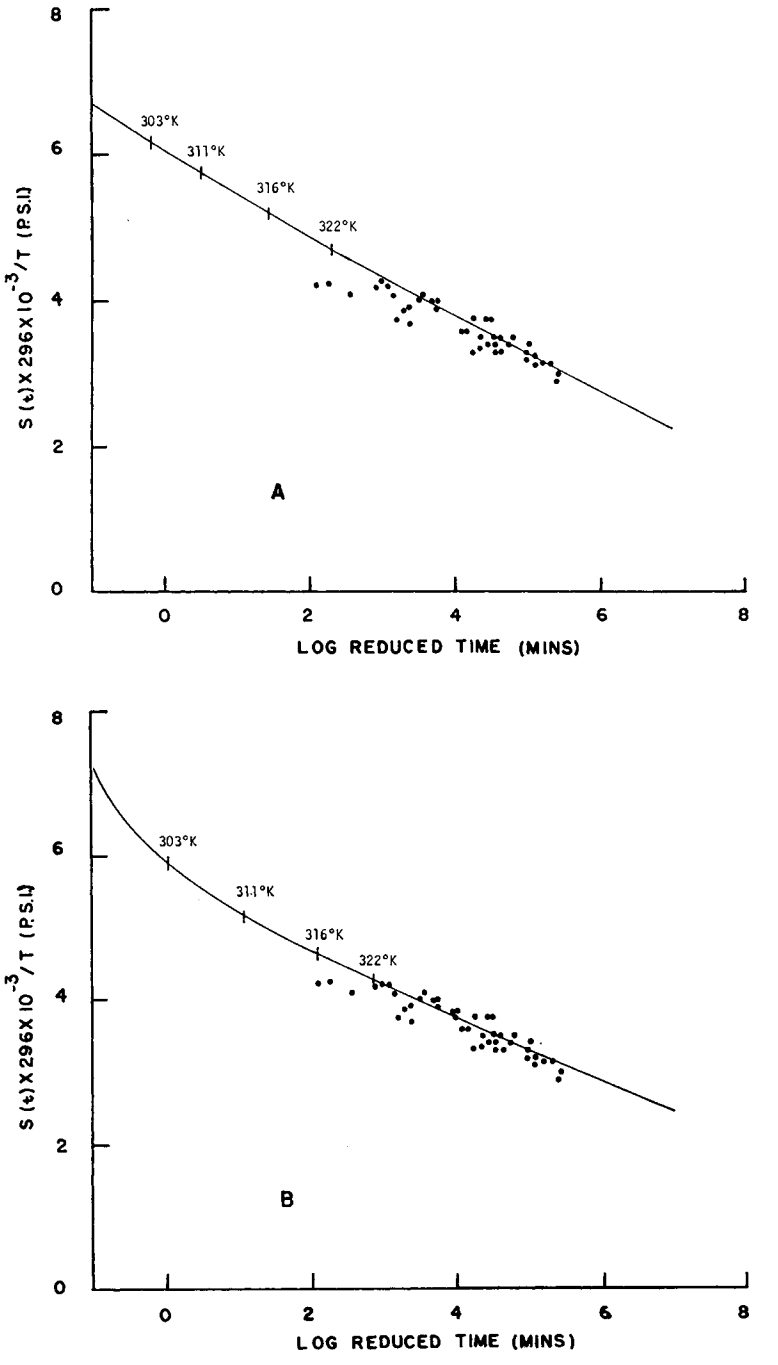

Fig. 9. Prediction of Barlow pipe-burst stress for (*A*) injection-molded and (*B*) compression-molded ABS II annealed for 12 hr. at 93°C.: (——) multiaxial pipe-burst prediction; (●) long-term Barlow pipe-burst data.

PREDICTION OF PIPE-BURST STRESS AT 23°C. FROM YIELD-STRAIN MASTER CURVES AT 23°C.

Figures 9*A* and 9*B* show the predicted curves of Barlow pipe-burst stress calculated by converting the uniaxial master-curve tensile data into multiaxial form. Actual Barlow pipe-burst stress data measured with two lots of ABS II pipe are plotted, to show the extent of agreement between predicted and measured 23°C. Barlow hoop stress up to 1.3×10^5 min.

Predictions of ISO pipe-burst data based on a short-term ISO pipe-burst stress of 6670 psi also have been made. Equally good agreement between measured and predicted pipe-burst stress is found, irrespective of whether the Barlow or ISO formula for pipe-burst stress is used. The different multiaxial converting factors used in compiling the predictions of both Barlow and ISO pipe-burst data are compared in Table IV.

TABLE IV
Comparison of ABS II Experimental Multiaxial Conversion Factors (MCF) with Theory

Tensile Specimen	Barlow (MCF)	ISO (MCF)
Annealed, injection-molded	1.03	0.93
Annealed, machined, compression-molded	1.14	1.03
von Mises theoretical	1.16	1.04

MELT EXTRUSION OF ABS I AND II

The apparent activation energies ΔH_a for melt flow have been calculated for the two ABS plastics based on the same diene, to determine whether differences mainly attributable to structural changes associated with the diene content exert the same influence on melt flow as are observed during stress relaxation at yield strain.

The apparent melt viscosities η_a of the two ABS plastics were measured from 200 to 300°C. as a function of apparent shear rate $\dot{\ }_a$ from 1.7 to 1740 sec.$^{-1}$. The log η_a dependence on $1/T$ was found to be linear at all shear rates for both resins, which verifies that ABS conforms to an Arrhenius melt-flow relationship,

$$\eta_a = A \exp \{-\Delta H_a/RT\}$$

which is controlled by an apparent activation energy ΔH_a.

The η_a versus γ_a^0 curves showed that ABS I had a higher η_a than ABS II at all shear rates and temperatures, and that the higher diene ABS I was more shear sensitive at a given temperature. Figure 10 shows that the ΔH_a of both plastics decays linearly with log $\dot{\gamma}_a$ except at the highest shear rates. ABS I has a lower ΔH_a over this linear region and shows a smaller ΔH_a decrease with increasing rate of shear. This means that the temperature dependence of η_a is less pronounced for the higher diene ABS and is less sensitive to shear rate. The ΔH_a values at 0.1 sec.$^{-1}$ of shear are

10 and 15 kcal./mole for ABS I and II, respectively, which compare with the corresponding ΔH_a values of 44 and 57 kcal./mole for stress relaxation at yieid strain at temperatures below the T_g of the rigid matrix. The melt ΔH_a values for ABS I and II are lower by 77 and 74%, respectively. The close similarity of these differences in ΔH_a, irrespective of diene content, is probably due to a similar increase in the mobility of the styrene–acrylonitrile copolymer chain segments on attaining the melt state. If this is the case, approximately 75% of the stress-relaxation activation energy can be attributed to the decrease of the copolymer segment mobility below

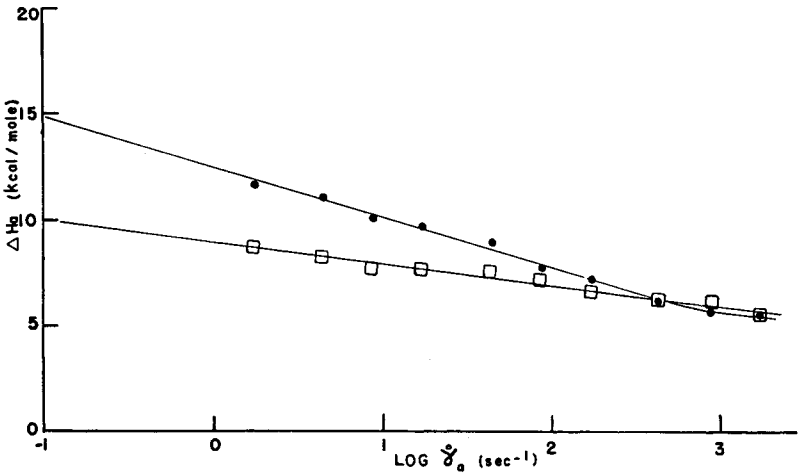

Fig. 10. Variation of apparent activation energy ΔH_a for melt flow with apparent shear rate $\dot{\gamma}_a$ from 200 to 300°C.: (□) ABS I; (●) ABS II.

its T_g. The activation energy for ABS molecular mobility may well be related to free volume and its response to strain. A higher diene content then provides more free volume to facilitate cold-flow in the rigid matrix below its T_g and also lowers the energy barrier to melt flow above T_g.

CONCLUSIONS

Semilogarithmic stress-relaxation curves are time–temperature superposable for the ABS system at strains from well within the linear viscoelastic limit to beyond yield. Stress relaxation ΔH_a and τ values support the observation that the relaxation rate increases to a maximum near yield strain and thereafter remains essentially unchanged up to break.

The stress–strain–reduced time surface provides a valuable basis for design and engineering with ABS plastics. From the master curves at linear strains tensile creep data can be computed for ABS plastics. The 23°C. hydrostatic pipe-burst strength of ABS plastics can be predicted successfully from stress-relaxation master curves at yield strain, if the temperature range has an upper limit of 40 °C. below the rigid-copolymer T_g.

Specimen preparation appears to be relatively unimportant for pipe-burst prediction, if the tensile stress-relaxation specimens are annealed for 12 hr. at the 264 psi ASTM heat-distortion temperature. ABS long-term pipe-burst strength improves as rubber content decreases and the fraction of load-bearing matrix in the cross-sectional area increases. The structural changes which occur as a result of increasing diene content are associated with a decrease in ΔH_a for both stress relaxation below the T_g of the rigid copolymer and melt flow above the copolymer T_g.

I wish to acknowledge the assistance of J. F. Sabol and C. R. Shingleton in preparing specimens and making the stress-relaxation measurements.

References

1. H. Leaderman, *Textile Res. J.*, **11**, 171 (1941); *ibid, Elasticity and Creep of Filamentous Materials*, Textile Found., Washington, D.C., 1963, pp. 16, 30, 76, 100.
2. A. V. Tobolsky, *Properties and Structure of Polymers*, Wiley, New York, 1960.
3. J. D. Ferry, *Viscoelastic Properties of Polymers*, Wiley, New York, 1960.
4. P. E. Rouse, Jr., *J. Chem. Phys.*, **21**, 1272 (1953).
5. A. Nadai, *Theory of Flow and Fracture of Solids*, Vol. I, 2nd Ed., McGraw-Hill, New York, 1950.
6. E. Baer, Ed., *Engineering Design for Plastics*, Polymer Science and Engineering Series, Reinhold, New York, 1964.
7. S. Turner, *Brit. Plastics*, **37**, 682 (1964).
8. A. A. McLeod, *Ind. Eng. Chem.*, **47**, 1319 (1955).
9. M. L. Williams, R. F. Landel, and J. D. Ferry, *J. Am. Chem. Soc.*, **77**, 3701 (1955).
10. F. Bueche, *J. Appl. Phys.*, **26**, 738 (1955); ibid., **24**, 423 (1953).
11. K. Deutsch, E. A. Hoff, and W. Reddish, *J. Polymer Sci.*, **13**, 565 (1954).
12. S. Iwayanagi and T. Hideshima, *J. Phys. Soc. Japan*, **8**, 368 (1953).
13. J. A. Roetling, *Polymer*, **6**, 615 (1965).
14. J. A. Faucher, *Trans. Soc. Rheol.*, **3**, 81 (1959).
15. K. Nagamatsu and T. Yoshitami, *J. Colloid Sci.*, **14**, 377 (1959).
16. T. Yoshitami, K. Nagamatsu, and K. Kosiyama, *J. Polymer Sci.*, **27**, 335 (1958).
17. S. Newman and S. Strella, *J. Appl. Polymer Sci.*, **9**, 2297 (1965).
18. R. F. Landel and P. J. Stedny, *J. Appl. Phys.*, **31**, 1885 (1960).
19. G. M. Martin, F. L. Roth, and R. D. Stiehler, *Trans. Inst. Rubber Ind.*, **32**, 189 (1956).
20. J. D. Ferry and R. A. Stratton, *Kolloid-Z.*, **171** (1960).
21. F. W. Reinhart, *ASTM Special Technical Publication*, No. **375**, 30–47 (1965).
22. E. Baer, J. R. Knox, T. J. Linton, and R. E. Maier, *J. Soc. Plastics Engrs.*, **16**, 396 (1960).
23. J. H. Faupel, *Modern Plastics*, **35**, 120 (1958); *ibid.*, **35**, 132 (1958).

Received February 27, 1967
Revised August 21, 1967